

RECENT RESULTS FROM A COMBINED DIODE-RF GUN

C. Gough,[#] M.Paraliev, S.Ivkovic, PSI, Switzerland

Abstract

For the SwissFEL project, a novel combined diode-RF electron gun was tested at PSI. Typically, electron bunches of 1-100 pC charge, 1-5 MeV energy and 2-0.2 $\mu\text{m-rad}$ emittance were produced and measured. The advantage of the combined gun is that diode geometry and emission surface can be changed readily. An adjustable depression for the photo emitting surface within the cathode was used to find an optimum operating point, although longitudinal dynamics seemed to limit the measured emittance. The movable PepperPot (PP) Emittance Measurement System performance was measured and an improved algorithm for measuring the resulting beamlet widths is described. The optimum PP-YAG separation was found by the trade-off between beamlet resolution and optical noise floor.

INTRODUCTION

The combined DC-RF electron gun test stand at PSI delivered many useful results [1] and the Emittance Monitor System (EMSY) was a key element [2]. The principle of emittance measurement with a PepperPot (PP) and a Yttrium-Aluminium-Garnet scintillator screen (YAG) is based on Ref.[3].

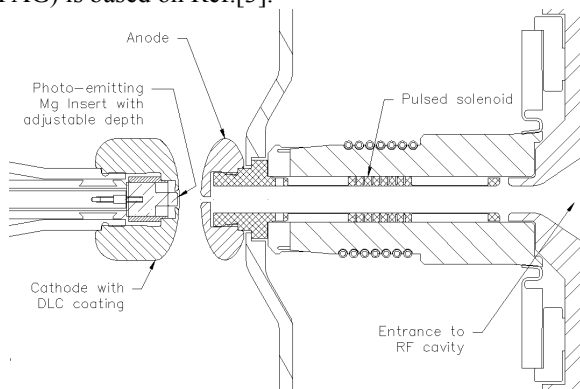


Figure 1: Diode cross section showing photo-emission surface with adjustable depth.

ADJUSTABLE CATHODE GEOMETRY

Fig.1 shows a modified cathode which allowed the depth of the Mg photo-emitting insert to be adjusted by stepper motor. The diode is driven by a pulsed voltage between 300-500 kV, and the following 2-cell 1.5 GHz cavity increased energy to 1-5 MeV. The curves in Fig.2 show results for an "optimum" depressed cathode setting. Fig.2 shows the geometric emittance plotted against the beam radius at the PP on the x-axis. This style of

[#] christopher.gough@psi.ch

presentation is useful when truncating the edges of PP images, since deviation from a straight line passing through the origin is a test for data consistency. The electron beam energy was ~ 5 MeV, so normalised emittance is found by multiplying the y-axis by $\gamma\beta \sim 10$. The PP image is interesting because, normal "comet tails" from energy dispersion evolved into circles using this particular cathode depression setting of 1.7 mm. The core beamlet is several times smaller than the projected ring shape. The curve gives a minimum emittance as the RF phase is swept. Sweeps of the RF phase with a range of cathode depressions gave insight into the interplay of charge, emission dynamics and local electric field on the cathode. One interpretation of the donut-shape PP beamlets is that high local charge and radial electric focusing are balancing at the cathode during the total emission interval (the laser pulse had a nominal sigma of ~ 3 ps, measurements at low gradient suggested time-smearred emission due to charge density limitations).

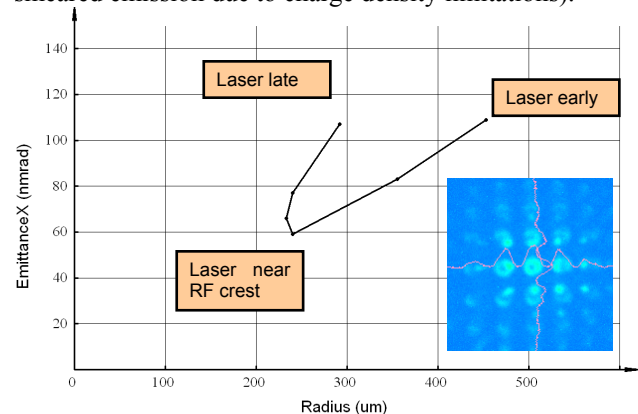


Figure 2: Geometric emittance against 1- σ beam radius, 50pC, with photo-emitting surface 1.7mm below cathode electrode surface.

PEPPERPOT RASTER AND THICKNESS

Using a transverse linear mover, sets of different PPs could be introduced into the electron beam for direct comparison. Table 1 summarises the emittance values found using a set of tungsten PPs with different hole sizes and rasters.

Table 1: Comparison of PP Plates from 200 μm Tungsten

	Hole Diameter	Hole Raster	Emittance X (100%)	Emittance X (80%)
PP #1	20 μm	150 μm	63nm-rad	43nm-rad
PP #2	20 μm	250 μm	84nm-rad	55nm-rad
PP #3	20 μm	250 μm	84nm-rad	51nm-rad
PP #4	50 μm	150 μm	67nm-rad	47nm-rad
PP #5	50 μm	150 μm	62nm-rad	44nm-rad
EMSY	50 μm	250 μm	84nm-rad	48nm-rad

From Table 1, the hole size had no effect. With the smaller raster, the beamlets tended to overlap on the image, leading to estimates of beam width that were too low, giving an artificially low emittance value. In general, a raster of 250 μm was reasonable with beam diameters around 1mm.

Fig.3 gives results for a set of four phosphor bronze PPs, mechanically drilled with a 120 μm holes, and the resulting beamlets analysed with the 2D ring fitting algorithm (described later in this paper). The four curves are peak normalised (<5%) to compensate for slightly different peak intensities. This shows that at this energy of ~ 4 MeV, almost any PP material is sufficient to scatter electrons so strongly that the emittance measurement is not degraded.

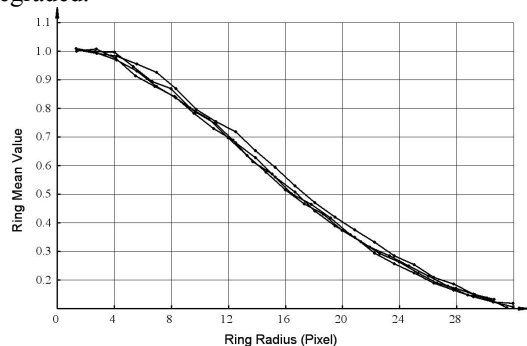


Figure 3: Beamlet profiles from phosphor bronze PP plates of four different thicknesses, 100 μm , 200 μm , 300 μm and 400 μm .

EMSY VISIBLE LIGHT OPTICS

A PCO Sencam camera with 6.45 μm pixel raster was used for these measurements (for other results in this paper, a Point Grey FL2-20S4M camera with 4.4 μm pixel raster was used). Fig.4 shows the layout of the EMSY. The visible optics resolution was measured by simulating the light emission from the YAG with a synthetic light source, built using a thin metal foil with 150 μm holes drilled in it, backed by a light diffuser, with red, green and blue LEDs. This light source was used in different locations in Fig.4. When the light source (or YAG) is upstream, the distance A is maximum and distance B is minimum; in this case the astigmatism from the asymmetric mirror mounting and the planarity of the vacuum window surfaces play a role comparable to the aberrations of the objective. However, when the distance B is large, mirror and window aberrations played a negligible role. The vacuum window finally used was a fused quartz Type 9722007 from MDC, with PbAg soldering. The best location (YAG towards the downstream end) gave the light profiles shown in Fig.5, approximated by a wide, raised cosine edge. Since the light source includes a diffuser, the expected edge resolution should be less than this value. At the same location, a 9 μm telecom glass fiber was installed, also with red, green and blue light. With this, the Point Spread

Function FWHM diameter was roughly 1pixel, considerably smaller than the edges shown in Fig.5.

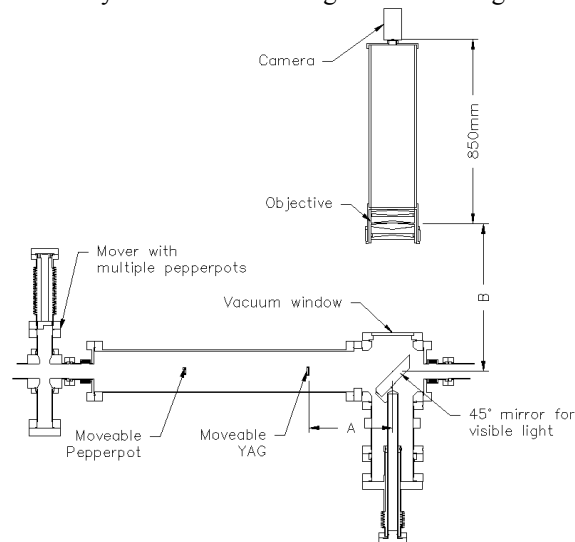


Figure 4: Schematic of the EMSY layout. The electron beam enters from the left. As the YAG position is changed by stepper motor, so is the camera and objective position so that the distance A+B is constant.

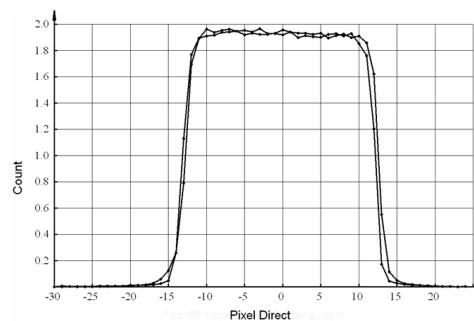


Figure 5: Best case edge resolution from large round hole projection, visible optics only, x and y directions.

BEAMLET WIDTH MEASUREMENT

Use of X and Y projections of the PP image did not give reproducible values of emittance. Two main problems were identified: the X or Y projection accumulated systematic noise and image distortion, and the beamlet width measurement using second moments was vulnerable to noise. A new algorithm was developed to analyse the PP images, not using simple 1D slicing or projections but rather by centering a series of 2D rings on each beamlet image. Fig.6 is a typical example. The integral around the ring can be imagined as the average of a large number of line profiles taken at many angles through the beamlet center, and in this sense gives the maximum possible Signal/Noise Ratio (SNR) for a small number of pixels.

A series of images were taken as the beam charge was varied, by varying the photo-emission laser energy. Fig.7

shows that all the high SNR beamlets within one image have the same width. Using low SNR beamlets as well is not useful since these increase the error band without changing the mean.

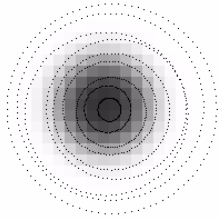


Figure 6: Example of fitted rings on a beamlet image.

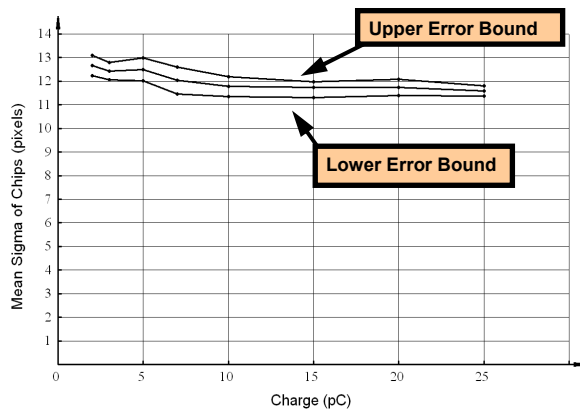


Figure 7: Fitted σ of dozens of individual beamlet profiles, using the 2D ring-fitting algorithm.

PEPPERPOT BEAMLET BEHAVIOUR

Fig.8 shows the beamlet profiles as the PP-YAG separation is changed but the unchanged electron beam. In this case, the profiles were narrower than normal due to beam convergence and did not fit so well to a Gaussian, but fitted better to the following equation:

$$Amplitude = A_{max} \exp(-k * s^3)$$

where $s = r / R_0$, R_0 and k are fitted constants and r is the radius from the beamlet center. When the PP and YAG are very close, the beamlet has high intensity and is narrow. In this case, the beamlet should have a trapezoid profile with a flat top and a width that matched the hole size diameter. As seen from Fig.8, the expected sharp edges are absent. We conclude that the $50\mu\text{m}$ Ce:YAG is dominating the beamlet resolution. Quantifying scintillator resolution is still an active field [4]-[7]. Fig.9 shows the result of an emittance calculation using the beamlets in Fig.8. With the PP closer than 100mm to the YAG, the beamlet width and emittance is over estimated. But with PP further than 250mm from the YAG, the weak outer beamlets are disappearing into the background

noise, so truncating the apparent electron beam diameter and giving the characteristic linear reduction of emittance.

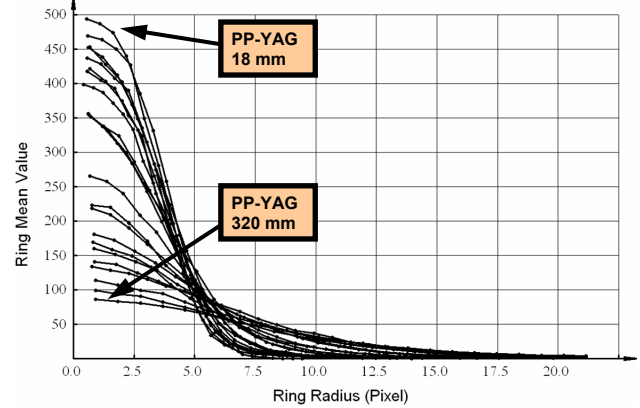


Figure 8: A beamlet spot profile with PP-YAG separation varying from 18 to 320mm.

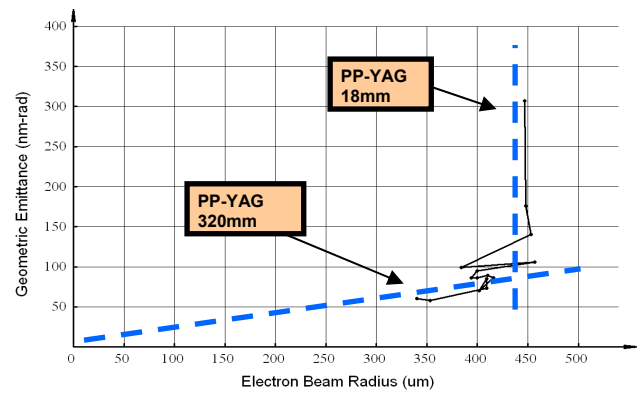


Figure 9: Emittance and beam radius as PP-YAG distance was varied from 18 to 320 mm.

SUMMARY

The adjustable cathode depression was used to find an optimum operating point. An improved method for pepperpot beamlet analysis was given and the inferred system resolution was limited by the YAG. The optimum PP-YAG separation is set by the trade-off between beamlet resolution and optical noise floor.

REFERENCES

- [1] R. Ganter et al., PRST-AB13 093502 (2010).
- [2] V. Schlott et al., DIPAC 2007, Venice.
- [3] S.G. Anderson et al., PRST-AB5, 014201(2002).
- [4] A. Murokh et al., in "The Physics of High Brightness Beams", 564-580, World Scientific Publishing 2000.
- [5] W.S. Graves W.S. et al., in 8th Beam Instrumentation Workshop, AIP 451, 206-213, 1998.
- [6] M. Kotera et al., Ultramicroscopy 54 (1994), 293-300
- [7] G. Kube et al, 906-8, Proc IPAC10, Kyoto.